ACS OMEGA

Open Access

http://pubs.acs.org/journal/acsodf

Article

Efficient Adsorption and Removal of the Herbicide 2,4-Dichlorophenylacetic Acid from Aqueous Solutions Using MIL-88(Fe)-NH_2

Ahmad A. Alluhaybi, Ahmed Alharbi, Khaled F. Alshammari, and Mohamed G. El-Desouky*

Cite This: *ACS Omega* 2023, 8, 40775−40784

Read Online

ACCESS | Metrics & More | Article Recommendations | Supporting Information

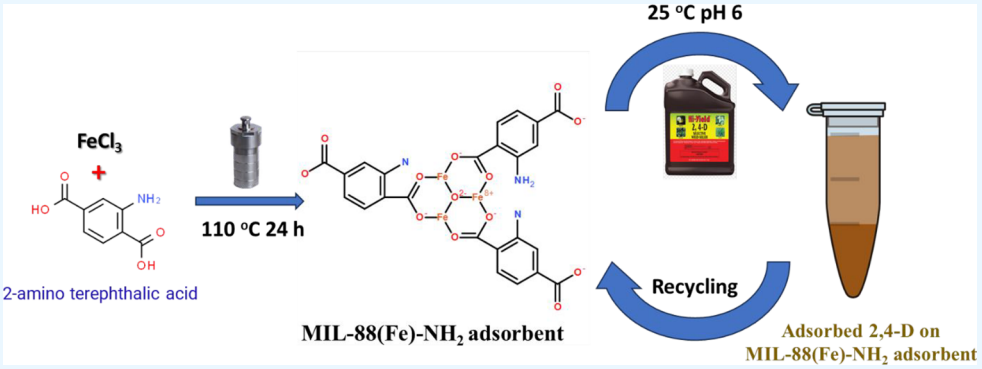

ABSTRACT: Metal−organic frameworks (MOFs), a material known for its multifunctionality, chemical stability, and high surface area, are now commonly utilized as an adsorbent for water treatment. The MOF (MIL-88(Fe)-NH_2) was synthesized and used to remove the commonly used toxic herbicide 2,4-dichlorophenoxyacetic acid (2,4-D) from water. The MIL-88(Fe)-NH_2 MOF was fully characterized using multiple techniques. A systematic investigation was conducted to evaluate the key parameters that impact the adsorption process, which include coexisting anions, adsorbent dosage, and solution pH. The adsorption isotherm was fitted using the Langmuir model, while the kinetics were fitted using pseudo-second-order. The adsorption process was both chemisorption and endothermic. The capacity for adsorption increased with rising temperatures. The MIL-88(Fe)-NH_2 adsorbent has a maximum adsorption capacity of 345.25 mg g^{-1} for removing 2,4-D, significantly higher than previous adsorbents used for this purpose. The adsorption mechanism could be ascribed to hydrogen bonding, pore filling, $\pi-\pi$ conjugations between the 2,4-D molecules and the MIL-88(Fe)-NH_2 adsorbent, and electrostatic interactions. Furthermore, the adsorption capacity of MIL-88(Fe)-NH_2 adsorbent showed only a slight decrease after five successive recycles, and it could be easily regenerated through solvent washing. When used in environmental water samples, especially those containing electronic wastes, the MIL-88(Fe)-NH_2 adsorbent demonstrated satisfactory adsorption capacity and reusability. The MIL-88(Fe)-NH_2 adsorbent is more practical and reusable and has better adsorption capacity and shorter equilibrium time compared to previously reported adsorbents.

1. INTRODUCTION

Wastewater contaminated with pesticides can have dangerous consequences for both humans and the environment. Some potential hazards include toxicity to aquatic life. Pesticides can be toxic to fish, insects, and other aquatic organisms. Accumulation of them in the food chain due to their introduction through wastewater can cause harm to the ecosystem.[1] Pesticides can contaminate surface water and groundwater sources, which can be used as drinking water. Drinking water contaminated with pesticides can result in severe health problems, including cancer, reproductive problems, and developmental issues.[2] When wastewater containing pesticides is used for irrigation, it can harm agricultural crops and reduce the yield. This can lead to economic losses for farmers and food shortages for the population.[3] Overuse of pesticides can lead to the development of resistance in pests, making them harder to control with the same pesticides. This can lead to the use of stronger and more toxic pesticides, which can have even more hazardous effects on human health and the environment. Environmental pollution can result from the long persistence of pesticides in the environment. They can also be transported over long distances through air and water, causing contamination in areas

Received: August 8, 2023
Accepted: October 2, 2023
Published: October 20, 2023

far from their original application.[4] To prevent these hazards, it is important to properly handle, treat, and dispose of wastewater containing pesticides. This can include using effective treatment methods to eliminate pesticides from wastewater before releasing it into the background or reusing it for nonpotable purposes. Additionally, reducing the use of pesticides and adopting alternative pest control methods can also help to minimize the hazards associated with their existence in wastewater.[5]

Exposure to pesticides can cause a wide range of acute and chronic illnesses in humans. Some of the types of illnesses that can result from the existence of pesticides include acute toxicity.[6] In severe cases, acute toxicity can cause respiratory failure, coma, and even death. There is a correlation between certain pesticides and an elevated risk of cancer in humans. Certain pesticides, including glyphosate, a widely used herbicide, have been classified as carcinogenic to humans. Exposure to pesticides can lead to reproductive and developmental problems in both males and females. For example, exposure to some pesticides has been linked to decreased fertility, miscarriage, stillbirth, and birth defects. Pesticides can affect the nervous system and lead to symptoms such as headache, dizziness, confusion, and seizures.[7] Exposure to pesticides can cause respiratory problems, particularly in agricultural workers who are frequently exposed to pesticides.[8] Symptoms can include shortness of breath, wheezing, and coughing. Pesticides can cause skin and eye irritation, particularly if they come into direct contact with the skin or eyes.[9] This can lead to symptoms, such as itching, redness, and swelling. It is important to note that the severity of pesticide-related illnesses can vary based on the kind of pesticide, the dose and duration of exposure, and individual factors such as age, health status, and genetic susceptibility. Taking steps to minimize exposure to pesticides, such as using protective equipment and adopting alternative pest control methods, can help to reduce the risk of illness.[8]

Pesticides are chemicals that are used to control pests, including insects, weeds, fungi, and rodents. There are many different types of pesticides, which can be classified based on their chemical structure, mode of action, and target pest. Some of the major types of pesticides include: Insecticides are pesticides used to control insects. They can be further classified into several subcategories, including organophosphates, carbamates, pyrethroids, and neonicotinoids, Herbicides are pesticides that are used to control weeds.[10] They can be classified into several subcategories based on their mode of action, including selective herbicides, which target specific plants, and nonselective herbicides, which can kill all types of plants. Fungicides are pesticides used to control fungal diseases. They can be classified into several subcategories based on their chemical structure and mode of action.[11]

In order to control weeds, the herbicide 2,4-D is extensively used in agricultural and nonagricultural settings. However, the use of 2,4-D can have negative effects on the environment and human health, which make the removal of this chemical important. Exposure to 2,4-D has also been linked to a range of other health effects, including reproductive and developmental problems, neurotoxicity, and endocrine disruption. Environmental contamination: 2,4-D can persist in the environment and can potentially contaminate soil, water, and air.[12] This can have negative impacts on wildlife and ecosystems as well as on human health through exposure to contaminated water and food. Overuse of 2,4-D can cause the development of resistance in weeds, making them harder to control with the same herbicide. 2,4-D can contaminate surface and groundwater sources, which can be used as drinking water.[13]

To eliminate 2,4-D from the environment, several methods can be used, including physical, chemical, and biological treatments. These methods can help to break down or remove chemicals from soil, water, and air. Additionally, reducing the use of 2,4-D and adopting alternative weed control methods, such as integrated pest management (IPM), can help to minimize the need for herbicides and reduce the negative impacts associated with their use. There are numerous methods that can eliminate 2,4-D from contaminated soil, water, and air.[12] These methods include: Biodegradation involves the use of microorganisms to break down 2,4-D into less harmful compounds. This method can be successful in removing 2,4-D from soil and water, but it can be slow and dependent on environmental conditions. Chemical oxidation involves the use of chemicals, such as persulfate, ozone, or hydrogen peroxide, to break down 2,4-D into less harmful compounds.[14] This method can be operational in eliminating 2,4-D from water, but it can be expensive and may produce harmful byproducts. Photodegradation implies the exploitation of light, such as ultraviolet (UV) light, to break down 2,4-D into less harmful compounds. This method can be effective in removing 2,4-D from water, but it can be slow and dependent on environmental conditions.[15] Adsorption involves the utilization of materials, for example, clay or activated carbon, to adsorb 2,4-D from contaminated water or air. This method can be effective in eliminating 2,4-D from low-concentration solutions and has the advantage of being cheap, simple, and environmentally friendly.[16] Adsorption techniques play a significant role in eliminating 2,4-D because they are effective, inexpensive, and eco-friendly. Adsorption can be used alone or in combination with other techniques to withdraw 2,4-D from contaminated water or air.[17]

MOFs are a porous material that is promising for adsorbing pollutants like 2,4-D. They have several advantages over traditional adsorbents, including high stability, surface chemistry, tunable pore size, and high surface area.[18] MOFs possess the ideal properties to effectively remove 2,4-D from contaminated water or air. Several studies have examined the adsorption of 2,4-D in MOFs. For example, a study found that a particular MOF, called MIL-101(Cr), was highly effective in removing 2,4-D from water. Another study published in the journal *Chemosphere* found that a different MOF, called UiO-66-NH_2, was effective in removing 2,4-D from aqueous solutions.[19] The application of MOFs for the adsorption of 2,4-D is a promising technique that has shown great potential in removing this herbicide from contaminated water or air. The unique properties of MOFs make them ideal candidates for the elimination of 2,4-D. In conclusion, MOFs are promising materials for the adsorption of 2,4-D from contaminated water or air. The unique properties of MOFs, including high stability, surface chemistry, tunable pore size, and high surface area, make them ideal candidates for the elimination of 2,4-D. However, further research is needed to optimize the adsorption conditions and regeneration methods for practical application. With the use of MOFs, we can mitigate the negative impacts of 2,4-D on human health and the environment.

MIL-88(Fe)-NH_2, also known as $Fe_3O(OH)(H_2N\text{-}bdc)_3$ or simply MIL-88-NH_2, is a fascinating and versatile metal–organic framework (MOF) material. MIL-88(Fe)-NH_2, in

https://doi.org/10.1021/acsomega.3c05818
ACS Omega 2023, 8, 40775−40784

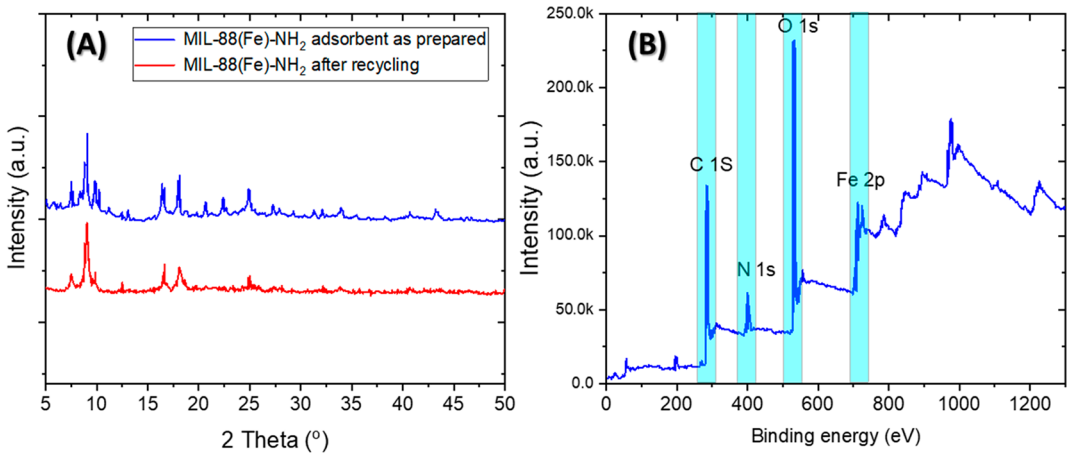

Figure 1. (A) XRD patterns of the MIL-88(Fe)-NH_2 adsorbent before and after reusing five times. (B) XPS survey scan spectrum of MIL-88(Fe)-NH_2 adsorbent.

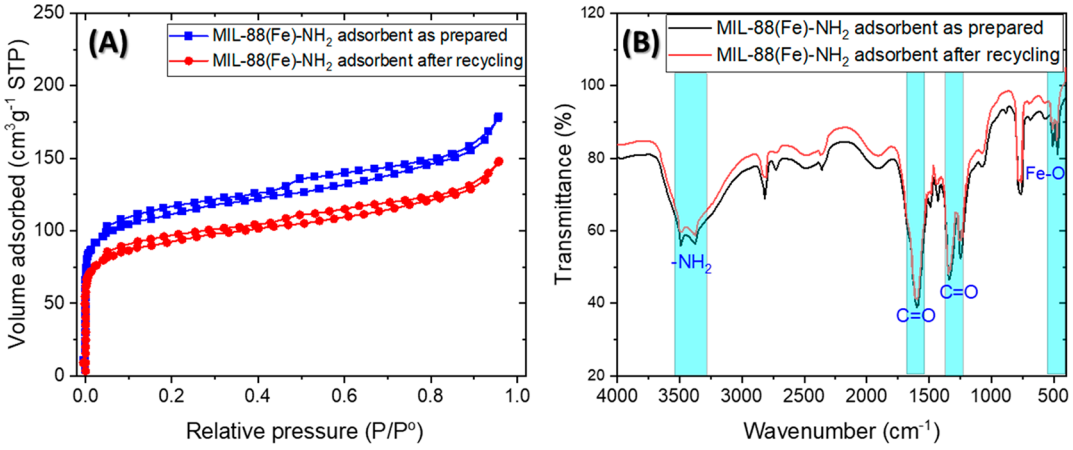

Figure 2. (A) BET sorption isotherms and (B) FT-IR spectra of the MIL-88(Fe)-NH_2 adsorbent before and after reusing five times.

particular, features iron (Fe) ions or clusters coordinated with amino-functionalized benzene-dicarboxylate (H_2N-bdc) ligands. In summary, MIL-88(Fe)-NH_2 is a remarkable metal−organic framework known for its high porosity and diverse applications, particularly in areas involving gas storage, catalysis, drug delivery, and sensing. Its unique structure and functionalization possibilities make it a promising material for addressing a wide range of challenges in science and technology.

The uniqueness of this study lies in the successful synthesis and characterization of MIL-88(Fe)-NH_2, which provides a high surface area and effectively removes harmful pesticide (2,4-D) from wastewater with high efficiency. On the contrary, the adsorbent can be reused up to five times. Our adsorbent was found to be more effective than others in removing 2,4-D, as per a comparison with previous studies.

2. EXPERIMENTAL SECTION

2.1. Materials. The Supporting Information provides detailed demonstrations of all materials and equipment that are used in this work.

2.2. Preparation of the MIL-88(Fe)-NH_2 Adsorbent. The MIL-88(Fe)-NH_2 was synthesized in a conventional way using the reported procedures.[20] Detailing the process, the first solution was formed by adding 1.242 mmol of 2-amino-terephthalic acid to 7.5 mL of dimethylformamide. The second solution was created by dissolving 2.497 mmol of $FeCl_3$ in 7.5 mL of dimethylformamide. A 30 mL autoclave was filled with a mixture of solution first and second. Washing MIL-88(Fe)-NH_2 twice with methanol and deionized water resulted in its acquisition after it was treated in a 110 °C oven for 24 h.

2.3. Removal Study Using the MIL-88(Fe)-NH_2 Adsorbent. The batch system was used to decontaminate 2,4-D from water. Experiments were conducted to examine the kinetics of adsorption at an initial concentration of 350 mg L^{-1} for 2,4-D. Isotherm tests were carried out at 293, 303, and 313 K with varying initial concentrations of 2,4-D (20−395 mg L^{-1}). The effects of salt ($NaHCO_3$, Na_2SO_4, NaCl, and $CaCl_2$), MIL-88(Fe)-NH_2 dosage (5, 7.5, 10, 15, 20 mg), contact duration (5 to 100 min), and pH value (2−10) on the removal of 2,4-D from aqueous solutions were studied. The testing involved adding 0.02 g of MIL-88(Fe)-NH_2 adsorbent to 25 mL of solution from 2,4-D at a pH value of 6 in an Erlenmeyer flask. While keeping the temperature constant, the flask was agitated on a thermostatic shaker with a constant rotational speed of 130 rpm for 100 min. The MIL-88(Fe)-NH_2 adsorbent loaded with 2,4-D was isolated by centrifugation after the adsorption process. Using a double-beam UV−vis spectrophotometer, the concentration of the 2,4-D supernatant was measured at 282 nm. Eqs 1 and 2 were used to determine the removal efficiency (% Re) at an equilibrium and adsorption capacity (q_e) of 2,4-D.[21]

https://doi.org/10.1021/acsomega.3c05818
ACS Omega 2023, 8, 40775−40784

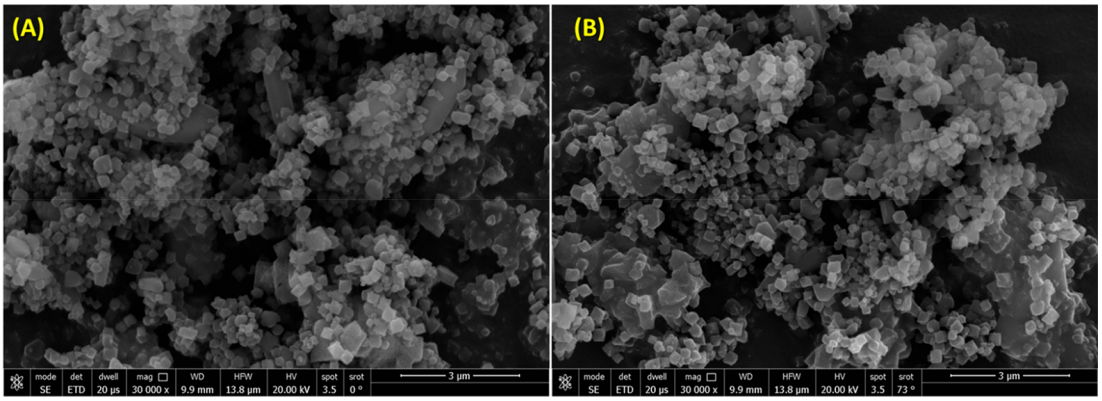

Figure 3. SEM image of MIL-88(Fe)-NH_2 (A) before adsorption and (B) after reusing five times.

$$\% \text{ Re} = \frac{(C_0 - C_t)}{C_0} \times 100 \quad (1)$$

$$q_e = \frac{(C_0 - C_e)V}{M} \quad (2)$$

3. RESULTS AND DISCUSSIONS

3.1. Characterization of MIL-88(Fe)-NH_2 Asorbent. *3.1.1. X-ray Dffraction (XRD).* The as-prepared MIL-88(Fe)-NH_2 adsorbents before and after reusing XRD patterns are shown in Figure 1. At approximately 9.1°, 12.7°, 12.9°, 16.6°, 18.5°, 20.7°, 25.0°, 26.3°, and 29.4°, the main diffraction peaks of both samples were observed. The diffraction peaks match those in published data on MIL-88-NH_2 single crystals, confirming that a pure product was obtained.[21] It is also indicated that the stability of the crystal structure of the MIL-88(Fe)-NH_2 adsorbent ramained even after multiple uses.

3.1.2. XPS. The occurrence of N, O, C, and Fe elements in the MIL-88(Fe)-NH_2 adsorbent sample was proven by the XPS survey spectrum, as shown in Figures 1B and S1. The 284.5 eV binding energy peak can be ascribed to the C 1s bond. The N 1s emission spectrum at 400.1 eV can be ascribed to C−N bonds. The O 1s emission spectrum appeared at 532.2 eV. Fe 2p1/2 and Fe 2p3/2 peaks were noted at 725.8 and 711.9 eV, respectively, indicating Fe^{3+} binding energy.[22]

3.1.3. N_2 Adsorption−Desorption Isotherm. The MIL-88(Fe)-NH_2 adsorbent's textural properties were evaluated using N_2 adsorption−desorption experiments, which were conducted before and after five rounds of reuse (Figure 2A). At intermediate relative pressure, the H4-type hysteresis loop was exhibited by the two samples with a type I curve. The MIL-88(Fe)-NH_2 adsorbent had a BET surface area of 437 m^2 g^{-1} before reuse, which decreased to 371 m^2 g^{-1} after reuse five times. The MIL-88(Fe)-NH_2 adsorbent's pore diameters were assigned as 0.98 and 0.83 nm before and after it was reused, respectively, where the Barret−Joyner−Halenda technique was used to estimate the sample's porosity (Figure 2). The MIL-88(Fe)-NH_2 adsorbent had a total pore volume of 0.13 cm^3 g^{-1} before reuse, which declined to 0.1 cm^3 g^{-1} after reuse, as shown in Figure S2. The reduce in the surface area, total pore volume, and the pore diameters of the reused MIL-88(Fe)-NH_2 adsorbent may be attributed to the holding of some molecules of 2,4-D on the surface and in the pores after each use.[22]

3.1.4. FT-IR. FT-IR spectroscopy was employed to characterize the MIL-88(Fe)-NH_2 adsorbent, as indicated in Figure 2B. It is clear from the spectra that vibrational bands of the —NH_2 groups can be seen at around 3485 and 3374 cm^{-1}. Protonated carboxylic groups, typically indicated by a band at around 1710 cm^{-1}, were not observed. The two carboxylic groups in the 2-aminoterephthalic acid were coordinated with Fe^{3+} after deprotonation, as suggested by the results. In-plane and out-of-plane bending of the carboxylic groups are the probable cause of the bands around 682 cm^{-1}.[23] Vibrations related to (O−Fe−O) appeared as bands at 552, 515, and 463 cm^{-1}.[23]

3.1.5. SEM Analysis. Figure 3 illustrates the SEM analysis conducted to examine the morphology of the MIL-88(Fe)-NH_2 adsorbent before and after being used five times. SEM images (Figure 3A) reveal that the MIL-88(Fe)-NH_2 adsorbent is made up of nanoparticles that are both nonaggregated and monodispersed. According to the images of the sample, cubic-shaped nanoparticles of varying sizes (250 to 390 nm) were observed.[24] After being used five times, the SEM images (Figure 3B) show that the morphology of the adsorbent remained mostly unchanged. This suggests that the adsorbent is stable and can withstand multiple uses without significant changes in its morphology. Moreover, the images show that the nanoparticles are still nonaggregated and monodispersed, indicating that the MIL-88(Fe)-NH_2 adsorbent can maintain its structural integrity even after repeated use. This is an important characteristic for an adsorbent as it ensures consistent performance over time.

3.1.6. Point of Zero Charge. The type of sorbent material and experimental synthesis conditions play a crucial role in the electrokinetic performance of the sorbent, as demonstrated by the measured pHzpc value. The MIL-88(Fe)-NH_2 has a positive surface charge when the pH value falls below pHzpc value 6.75, causing 2,4-D to be negatively charged and attracted to it. This leads to favorable adsorption below pH value 6.75, while repulsion occurs above it due to negative charge formation, according to Figure 4.[25]

3.2. Batch Experiments. *3.2.1. Effect of pH.* The adsorption process benefits from adjusting the pH value of the medium. Adsorbate nature and the adsorbent surface charge can be influenced by the solution pH value. 2,4-D (pK_a = 2.98) has the ability to exist as molecular or ionized forms in solution. The illustration in Figure 5 displays how 2,4-D binds to polymers under varying pH levels, ranging from 2 to 12. This relates to the characteristics of the MIL-88(Fe)-NH_2 adsorbent, whose pH_{pzc} value is 6.75. According to the result, the pH value of 6 was the optimum range for extracting 2,4-D from aqueous solution. Ionic interaction between 2,4-D and the sorbent is influenced by the pH value. The −NH_2 group of

https://doi.org/10.1021/acsomega.3c05818
ACS Omega 2023, 8, 40775−40784

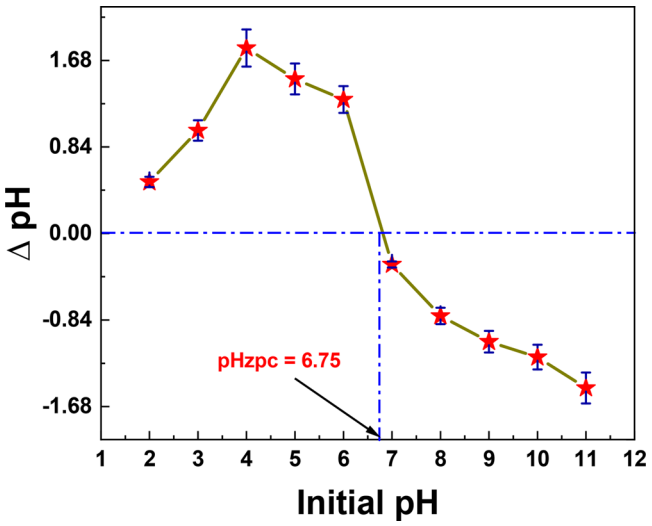

Figure 4. pH of zero negative discharge of the MIL-88(Fe)-NH_2 adsorbent.

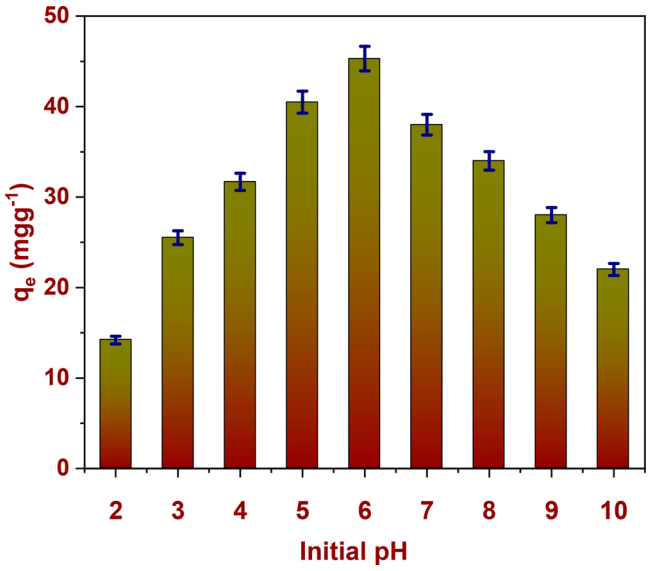

Figure 5. Impact of pH on the adsorption of 2,4-D using the MIL-88(Fe)-NH_2 adsorbent.

the sorbent becomes protonated in a strong acid solution, whereas the ionized forms of 2,4-D in alkaline solution do not aid in adsorption. Hence, the solution's pH was set to 6.0 for the subsequent adsorption examination.[26] As the capacity of the MIL-88(Fe)-NH_2 adsorbent to take up anionic 2,4-D adsorbate was increased, its surface characteristics improved when extra H^+ ions were found in the medium at minimal pH value. When the pH value is increased, the hydroxide ions increase and cause the creation of oxide-containing species on the MIL-88(Fe)-NH_2 adsorbent surface. The adsorption efficiency of the MIL-88(Fe)-NH_2 adsorbent is decreased by these species that impede the interaction of functional sites with 2,4-D. All adsorption experiments in this study utilized a pH value of 6 continuously.[27]

3.2.2. Effect of Dose. Sufficient active sites for adsorbate removal depend on the adsorbent dosage, making it a basis factor in the adsorption process.[28] At 293 K, the effect of the MIL-88(Fe)-NH_2 adsorbent dose on the adsorption of 50 mg L^{-1} of 2,4-D was studied using 0.02 to 0.25 g of the adsorbent dosages. The increase of the MIL-88(Fe)-NH_2 adsorbent mass from 0.02 to 0.25 g improved the percentage removal (% R) of 2,4-D solution from 57.9% to 97.6%, as shown in Figure 6.

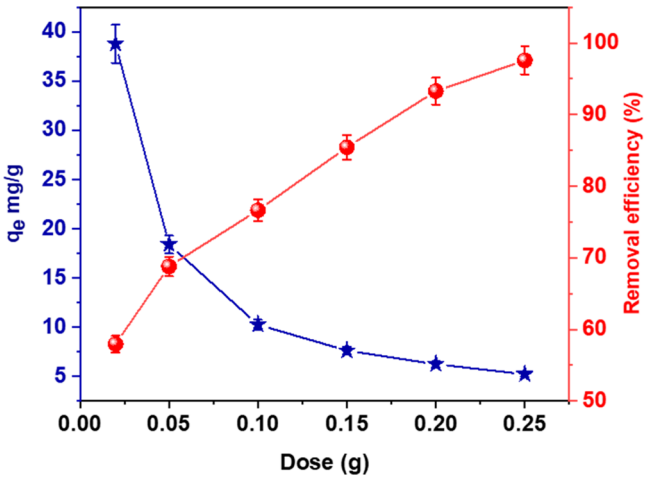

Figure 6. Effect of dose of MIL-88(Fe)-NH_2 adsorbent on adsorption of 2,4-D.

However, at a lower adsorbent dosage, the uptake of 2,4-D onto the MIL-88(Fe)-NH_2 adsorbent was higher, while it decreased from 22.5 to 1.3 mg g^{-1} as the dosage increased. The explanation for this is a higher adsorbent dosage, which results in most of the functional sites being occupied and lower uptake.

3.2.3. Adsorption Isotherm. There are several types of adsorption isotherms, including Langmuir,[29] Freundlich,[30] Dubinin−Radushkevich,[31] Temkin,[32] Jovanovic, and Redlich-Peterson.[33] Each of these isotherms has its own unique mathematical form and describes different aspects of the adsorption process.

In general, the procedure of different adsorption isotherms is foremost for understanding the mechanisms of adsorption and optimizing the design of the adsorption processes. Each isotherm gives unique data on the adsorption process and can identify the best adsorbent material and operating conditions for a particular application.[34] The adsorption isotherm models of 2,4-D onto the MIL-88(Fe)-NH_2 adsorbent are presented in Figure 7. Table S1 contains the isotherm parameters.

Increasing the initial 2,4-D concentrations resulted in a growth of MIL-88(Fe)-NH_2's loading capabilities. The exhaustion of adsorptive sites on the MIL-88(Fe)-NH_2 adsorbent surface and the concentration accretion of the initial 2,4-D lead to an increase in loading capacity. The exact opposite happened as the removal effectiveness decreased with increasing 2,4-D concentrations. Langmuir proved to be a more consistent isotherm model than the others as per the data analysis. The actual and theoretical loading capacity values' correspondence, along with the increased R^2, supported this. Each presented study confirmed the monolayer and homogeneous adsorption form of the MIL-88(Fe)-NH_2 adsorbent surface. The Temkin model suggests that, as the adsorbent becomes saturated, the adsorption energy will decrease in a linear fashion, in contrast to the Freundlich pattern (characterized by Temkin constants A and B). The strong interaction of 2,4-D molecules with the MIL-88(Fe)-NH_2 adsorbent surface is shown by the high A and B values of 65.68 L g^{-1} and 1.73 kJ mol^{-1}. The adsorption energy of 17.82

https://doi.org/10.1021/acsomega.3c05818
ACS Omega 2023, 8, 40775−40784

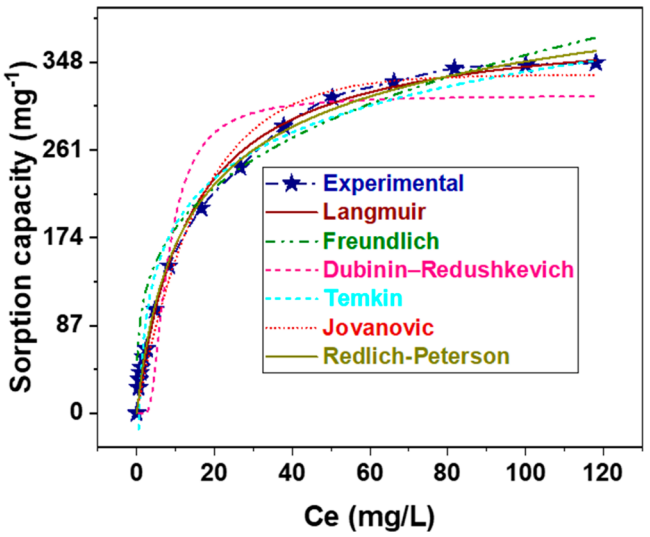

Figure 7. Adsorption isotherm models of 2,4-D onto the MIL-88(Fe)-NH_2 adsorbent.

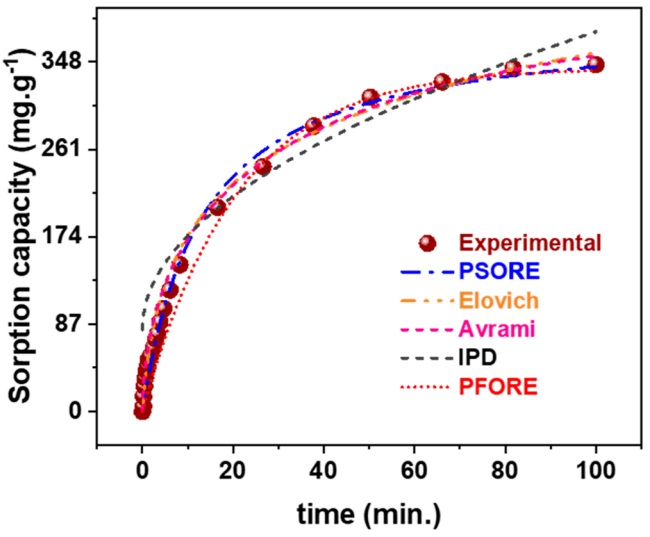

Figure 8. Adsorption kinetic models of 2,4-D onto the MIL-88(Fe)-NH_2 adsorbent.

kJ mol^{-1} from Dubinin−Radushkevich proved the chemisorption nature of the adsorption process.[35]

3.2.4. Adsorption kinetics. The rate at which a solute is adsorbed onto a surface can be described using mathematical equations called adsorption kinetic models. There are several types of adsorption kinetic models, like pseudo-First-order kinetic (PFORE),[36] pseudo-second-order kinetic (PSORE),[37] intraparticle diffusion (IPD),[38] Elovich,[39] and Avrami. Each of these models has its own unique mathematical form and describes different aspects of the adsorption process. To gain insights into the mechanisms of adsorption and optimize adsorption processes, it is important to employ adsorption kinetic models. The application of diverse adsorption kinetic models is crucial to comprehending adsorption mechanisms and improving adsorption process design. The models offer distinct insights into the adsorption process and can help to find the most suitable adsorbent material and operating conditions for a specific use. Figure 8 illustrates the kinetic models of adsorption of 2,4-D onto the MIL-88(Fe)-NH_2 adsorbent. Table S2 contains the calculated kinetic parameters.

PFORE, PSORE, IPD, and Elovich models were used to assess the impact of interaction time and order on the diffusion rate of 2,4-D and the controlling step in adsorption kinetics. PSORE suggested that the adsorption process is controlled by electron transfer or sharing between the adsorbent and adsorbate surface, while assuming that the rate is proportional to the difference between q_e and q_t. Figure 8 demonstrates the accurate assessment of the model's adequacy through the use of nonlinear regression. The conclusion is easily drawn that the PSORE model was the most suitable for matching the results of 2,4-D adsorption onto MIL-88(Fe)-NH_2 by comparing R^2 values in Table S2 and Table S3.[40]

Three main processes must be undergone by the adsorbate to move from bulk solution to the solid surface as per theory. (i) The MIL-88(Fe)-NH_2 surface (film diffusion) receives 2,4-D molecules from the bulk solution externally. (ii) Diffusion of 2,4-D molecules through MIL-88(Fe)-NH_2 pores leads to intraparticle diffusion and occupation of adsorptive sites. The regular distribution of 2,4-D molecules on the surface of positively charged MIL-88(Fe)-NH_2 leads to strong binding. To investigate the rate-limiting steps in the adsorption process of 2,4-D, researchers employed the IPD model (Figure 9). The adsorption process on a porous adsorbent consists of three

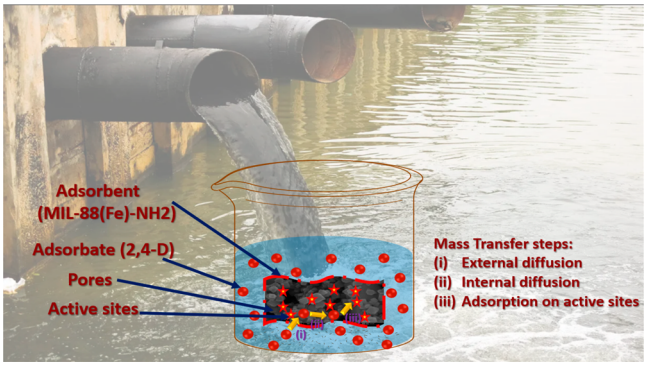

Figure 9. Diffusion mechanism of 2,4-D onto MIL-88(Fe)-NH_2.

primary stages: mass transfer through the liquid film outside, movement of adsorbate molecules within the particle, and attachment to the internal or external sites of the adsorbent through physical or chemical bonding. The adsorption rate is expected to be most affected by film or intraparticle diffusion, given the assumption that the final step is rapid. To understand the adsorption process mechanism, q_t was plotted against $t^{0.5}$ by modifying IPD. IPD is the sole regulation mechanism for adsorption if the illustrated line equals zero mathematically, as indicated here. In the event that the source is unsuccessful, other approaches, such as liquid film diffusion, can be used to handle the adsorption process. The behavior of the multilinear plots of q_t versus $t^{0.5}$ can be primarily divided into three linear zones, as shown in Figure 8. The rate of the adsorption process did not seem to be limited by intraparticle diffusion. The increased rate constants in the first stage could be due to the exterior film diffusion of the MIL-88(Fe)-NH_2 adsorbent. The equilibrium stage follows progressive intraparticle diffusion, as confirmed by negative X values in stage one. The diffusion in meso- and micropores regulates uptake kinetics during later stages. The Elovich equation was introduced to explain how adsorption energies vary among adsorptive sites, which are linked to their heterogeneous nature. The excellent efficiency

https://doi.org/10.1021/acsomega.3c05818
ACS Omega 2023, 8, 40775−40784

of MIL-88(Fe)-NH_2 toward 2,4-D is clearly indicated by the anticipated initial adsorption (α) and desorption (β) rates of 59.29 and 0.012 g $mmol^{-1}$ for 2,4-D, which are perfectly presented in Table S2.[41]

3.2.5. Adsorption Thermodynamics. To comprehend the sorption process, the impact of environmental temperature on the sorption profile of 2,4-D onto the MIL-88(Fe)-NH_2 adsorbent was analyzed at multiple temperatures. At elevated temperatures, the affinity of the MIL-88(Fe)-NH_2 adsorbent for 2,4-D increased significantly, with the equilibrium sorption capacity rising from 301.2 mg g^{-1} (RE % = 62.9%) to 401.7 mg g^{-1} (RE % = 93.8%) as the temperature rises from 293 to 323 K. By utilizing the MIL-88(Fe)-NH_2 adsorbent, the endothermicity of 2,4-D sorption is confirmed in an intuitive manner. The MIL-88(Fe)-NH_2 adsorbent has a high tendency for 2,4-D molecules, which is enhanced at higher temperatures due to a thinner boundary layer and increased binding activity. Figure 10 suggests that the movement of 2,4-D molecules, interaction with free binding centers, and their diffusion within sorbent pores were facilitated.[42,43]

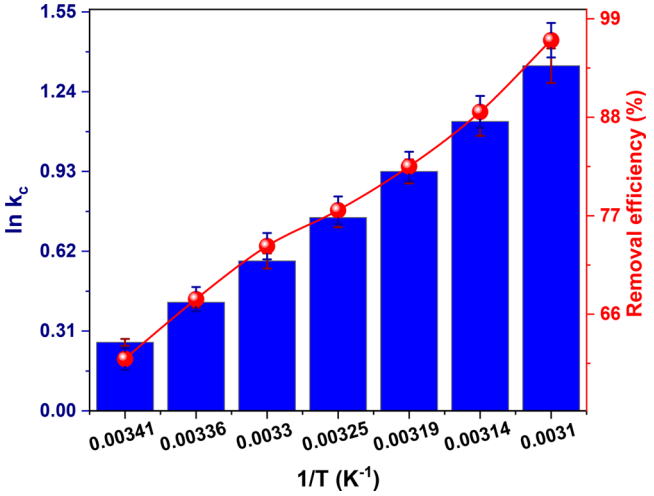

Figure 10. Influence of temperature on the 2,4-D adsorption onto the MIL-88(Fe)-NH_2 adsorbent

The sorption mechanism of 2,4-D molecules onto the MIL-88(Fe)-NH2 adsorbent can be explained through thermodynamics studies.[44]

Equation S1 was employed to calculate K_c, the adsorption equilibrium constant, which was then used in combination with the van't Hoff equation S2 and traditional thermodynamic equations S3 and S4 to assess the sorbent's thermodynamic constants.

By observation of the plot of ln K_c versus $1/T$, as depicted in Figure 9, the slope and intercept can be used to find the values of thermodynamics functions for the adsorption process, and the results are displayed in Table S4. The spontaneous nature of 2,4-D sorption onto the MIL-88(Fe)-NH_2 adsorbent increases with elevated temperatures, indicating a decrease in $\Delta G°$ values from 298.0 to 328.0 K. The endothermic sorption of 2,4-D onto the MIL-88(Fe)-NH_2 adsorbent was confirmed by the positive value of $\Delta H°$. From Table S4, the $\Delta H°$ value was 27.9 kJ mol^{-1}. The randomness system of sorption increased during the equilibrium of 2,4-D sorption onto the MIL-88(Fe)-NH_2 adsorbent, as evidenced by the positive $\Delta S°$ value of 97.11 J mol^{-1} K^{-1}.

3.2.6. Mechanism of Interaction. The possibility of cation interactions in n−π interactions is expected due to the presence of an aromatic ring in the structure of both the MIL-88(Fe)-NH_2 adsorbent and the 2,4-D molecule. Moreover, it is expected that conventional hydrogen bonds will be formed between the neutral 2,4-D and adsorbent. The −NH_2 could also interact with the OH of 2,4-D and create a hydrogen bond to aid in the removal of 2,4-D. However, as depicted in Figure 2, the surface area and pore volume decreased after adsorption, suggesting that some adsorption took place within the pores of the adsorbent. The potential interactions between the MIL-88(Fe)-NH_2 adsorbent and the 2,4-D are summarized in Figure 11.[45,46]

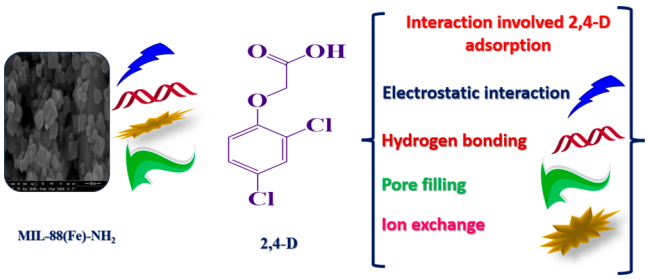

Figure 11. Mechanism of interaction between the MIL-88(Fe)-NH_2 adsorbent and the 2,4-D molecule.

3.2.7. Effect of Salinity. The presence of competing molecules or ions in effluents from industry makes the influence of ionic strength on sorption processes highly important. The MIL-88(Fe)-NH_2 adsorbent showed 96.13% RE with 2,4-D at the lowest NaCl concentration (5.0 g L^{-1}) which decreased as the NaCl concentration increased, as shown in Figure 12. The following various mechanisms can be used to show this inhibitory phenomenon: (i) Competition between background electrolytes such as Na^+ and Cl^- and 2,4-D lowers the electrostatic potential of the MIL-88(Fe)-NH_2 adsorbent surface, (ii) the MIL-88(Fe)-NH_2 adsorbent surface repels 2,4-D due to the compression of the double electric

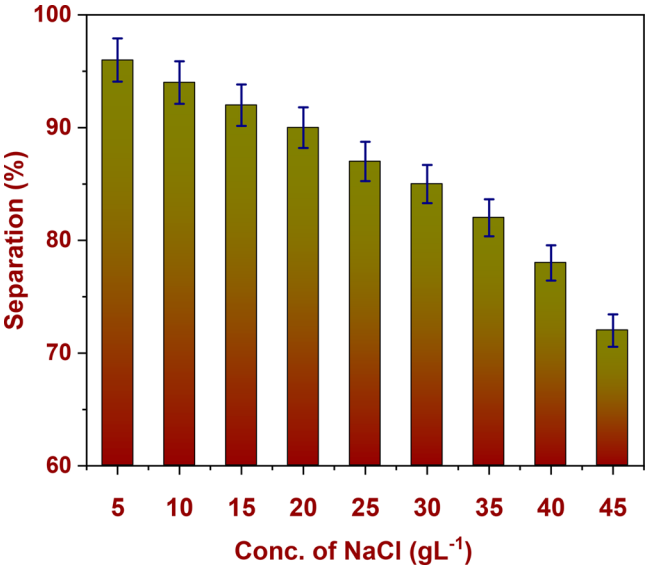

Figure 12. Impact of concentration of NaCl (ionic strength) on 2,4-D sorption.

https://doi.org/10.1021/acsomega.3c05818
ACS Omega 2023, 8, 40775−40784

layer and electrostatic forces, and (iii) the activity coefficient of 2,4-D in the solution is greatly affected by the ionic strength. However, the MIL-88(Fe)-NH_2 adsorbent's potential for further wastewater treatment applications was demonstrated through the unexpected validation of its resistance to ionic interference.[47,48]

3.2.8. Removal of the 2,4-D from Real Water Samples. The sorption performance of MIL-88(Fe)-NH_2 was assessed against real aqueous matrices to verify its practicality as a toxic collecting material such as 2,4-D, bearing in mind the system's complexity as a result of its many components (like biological constituent, natural minerals, organic matters, and inorganic cations/anions). The MIL-88(Fe)-NH_2 adsorbent was used to treat the wastewater sample. The 2,4-D was effectively captured from actual effluents (wastewater from farm at the port, Egypt) by the MIL-88(Fe)-NH_2 adsorbent with minimal loss in removal efficiency (RE %), from 88.61% (e.g., 5.0 mg L^{-1} of 2,4-D concentration) to 74.6% (e.g., 20.0 mg L^{-1} of 2,4-D concentration). The outcomes validated the remarkable effectiveness of cost-effective MIL-88(Fe)-NH_2 adsorbent in polluted industrial situations.[27,49]

3.2.9. Reusability. A used sorbent's ability to absorb gradually decreases during the sorption process until it is completely depleted. The regeneration scenario of the saturated sorbent determines the economic and environmental benefits of future practical applications. Table 1 and Figure 13 display the results of an evaluation of the desorption property of the MIL-88(Fe)-NH_2 adsorbent. It experienced a decrease in RE % to 84.4% after 5 cycles of sorption−desorption. The reduction in RE % was possibly due to several reasons, including the loss of sorbent material, deformation in the MIL-88(Fe)-NH_2 adsorbent network, and blockage of functional molecules on occupied adsorbent surfaces. However, the MIL-88(Fe)-NH_2 adsorbent demonstrated a significantly higher recyclability (84.4% regeneration efficiency) after the fifth cycle than other sorbents. For industrial wastewater treatment applications,[43,45,47,50] the regenerated MIL-88(Fe)-NH_2 adsorbent can be suggested as a highly convenient and cost-effective material due to its admirable adsorbability, rapid RE % rate, and high sorption capacity.

Table 1. Five Re-adsorption Cycles of the 2,4-D onto the MIL-88(Fe)-NH_2 Adsorbent Surface

Cycle	q_e (adsorption) (mg g^{-1})	q_e (desorption) (mg g^{-1})	Des. (%)
Cycle 1	348.56	342.28	98.2
Cycle 2	342.28	320.44	93.62
Cycle 3	320.44	294.2	91.82
Cycle 4	294.2	256.84	87.3
Cycle 5	256.84	216.77	84.4

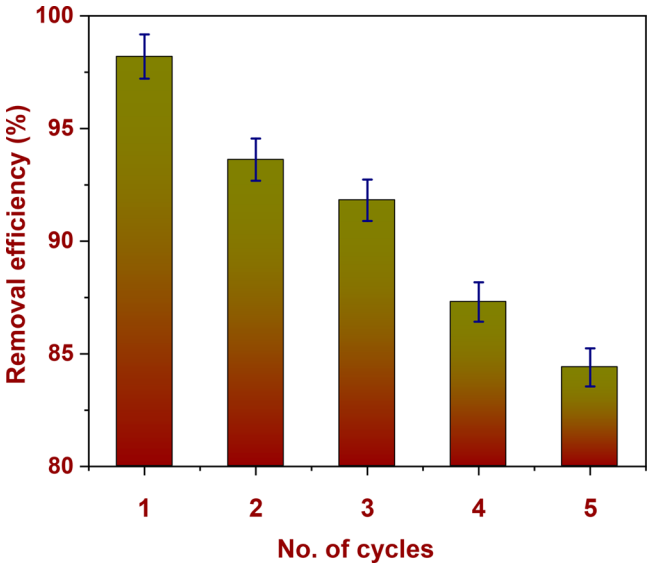

Figure 13. Reusability of MIL-88(Fe)-NH_2 adsorbent.

3.2.10. Comparative Analysis with Other Adsorbents. Table S5 contrasts the MIL-88(Fe)-NH_2 adsorbent's maximal sorption capabilities with a number of values taken from the literature. The challenge of directly comparing the sorption performance arises from varying experimental setups. It should be noted that the MIL-88(Fe)-NH_2 adsorbent has a significant advantage due to its quick kinetics. The strong MIL-88(Fe)-NH_2 adsorbent sorption capacity toward 2,4-D suggests that the sorbent may be useful in removing 2,4-D from wastewater.

4. CONCLUSION

In this study, MIL-88(Fe)-NH_2 was synthesized, examined, and used for adsorbing 2,4-D from aqueous environments. Based on the characterization analysis, it was determined that the surface area was 437 m^2 g^{-1}, which is high. Also, it was observed that a pH value of 6 and an adsorbent mass of 0.8 g per liter of solution were effective conditions for atrazine adsorption. At 298 K, the equilibrium data was best modeled by the Langmuir model with a maximum adsorption capacity of 445.25 mg g^{-1}, and the kinetics were in line with the pseudo-second-order. Adsorption mechanisms included surface adsorption through hydrophobic and $\pi-\pi$ interactions, as well as pore filling. The 445.25 mg g^{-1} of 2,4-D removal capacity can be reached under ideal conditions with synthesized MIL-88(Fe)-NH_2 adsorption. The adsorbent can go through five cycles based on its regeneration efficiency. The study showed that synthetic MIL-88(Fe)-NH_2 can serve as a more affordable substitute adsorbent for eliminating 2,4-D.

■ ASSOCIATED CONTENT

Supporting Information

The Supporting Information is available free of charge at https://pubs.acs.org/doi/10.1021/acsomega.3c05818.

Details for materials, instruments, and figures. Figure S1. XPS survey scan spectrum of (A) C 1s, (B) N 1s, (C) O 1s, and (D) Fe 2p in the MIL-88(Fe)-NH_2 adsorbent. Figure S2. Pore size distribution curve of the MIL-88(Fe)-NH_2 adsorbent before and after reusing for five times. Table S1. The isotherm parameters of adsorption of 2,4-D on MIL-88(Fe)-NH_2 adsorbent. Table S2. Adsorption kinetic parameters of 2,4-D on MIL-88(Fe)-NH_2 adsorbent. Table S3: List of abbreviations (PDF)

■ AUTHOR INFORMATION

Corresponding Author

Mohamed G. El-Desouky − *Egyptian Propylene and Polypropylene Company, Port Said 42511, Egypt;* orcid.org/0000-0001-6060-463X; Email: mohamed.eldesoky@EPP-EG.com, ch.moh.gamal@gmail.com

https://doi.org/10.1021/acsomega.3c05818
ACS Omega 2023, 8, 40775−40784

Authors

Ahmad A. Alluhaybi − *Department of Chemistry, College of Science and Arts, King Abdulaziz University, 25732 Rabigh, Saudi Arabia*

Ahmed Alharbi − *Department of Chemistry, Faculty of Sciences, Umm Al-Qura University, 21955 Makkah, Saudi Arabia;* orcid.org/0000-0002-1863-4672

Khaled F. Alshammari − *Department of Criminal Justice and Forensics, King Fahad Security College, 11461 Riyadh, Saudi Arabia*

Complete contact information is available at: https://pubs.acs.org/10.1021/acsomega.3c05818

Notes

The authors declare no competing financial interest.

■ ACKNOWLEDGMENTS

The authors extend their appreciation to the Deputyship for Research & Innovation, Ministry of Education in Saudi Arabia for funding this research work through the project number: IFP22UQU4331270DSR048.

■ REFERENCES

(1) Yang, X.; Muhammad, T.; Yang, J.; Yasen, A.; Chen, L. In-situ kinetic and thermodynamic study of 2, 4-dichlorophenoxyacetic acid adsorption on molecularly imprinted polymer based solid-phase microextraction coatings. *Sensors and Actuators A: Physical* **2020**, *313*, 112190.

(2) Wang, J.; Xu, Q.; Xia, W. W.; Shu, Y.; Jin, D.; Zang, Y.; Hu, X. High sensitive visible light photoelectrochemical sensor based on in-situ prepared flexible Sn3O4 nanosheets and molecularly imprinted polymers. *Sens. Actuators, B* **2018**, *271*, 215−224.

(3) Wang, H.; Wang, J.; Wang, J.; Zhu, R.; Shen, Y.; Xu, Q.; Hu, X. Spectroscopic method for the detection of 2, 4-dichlorophenoxyacetic acid based on its inhibitory effect towards catalase immobilized on reusable magnetic Fe3O4-chitosan nanocomposite. *Sens. Actuators, B* **2017**, *247*, 146−154.

(4) Lin, C.; Qiu, Y.; Fan, J.; Wang, M.; Ye, L.; Liu, Y.; Ye, X.; Huang, X.; Lv, Y.; Liu, M. Fabrication of photo-responsive cellulose based intelligent imprinted material and selective adsorption on typical pesticide residue. *Chem. Eng. J.* **2020**, *394*, 124841.

(5) Essandoh, M.; Wolgemuth, D.; Pittman, C. U., Jr; Mohan, D.; Mlsna, T. Phenoxy herbicide removal from aqueous solutions using fast pyrolysis switchgrass biochar. *Chemosphere* **2017**, *174*, 49−57.

(6) Rippy, M. A.; Deletic, A.; Black, J.; Aryal, R.; Lampard, J.-L.; Tang, J. Y.-M.; McCarthy, D.; Kolotelo, P.; Sidhu, J.; Gernjak, W. Pesticide occurrence and spatio-temporal variability in urban run-off across Australia. *Water research* **2017**, *115*, 245−255.

(7) Wang, X.; Yu, J.; Wu, X.; Fu, J.; Kang, Q.; Shen, D.; Li, J.; Chen, L. A molecular imprinting-based turn-on ratiometric fluorescence sensor for highly selective and sensitive detection of 2, 4-dichlorophenoxyacetic acid (2, 4-D). *Biosens. Bioelectron.* **2016**, *81*, 438−444.

(8) Gonzalez, A. E.; Asomoza, M.; Solis, S.; Sanchez, M. A. G.; Cipagauta-Diaz, S. Enhanced photocatalytic degradation of the herbicide 2, 4-dichlorophenoxyacetic acid by Pt/TiO 2−SiO 2 nanocomposites. *Reaction Kinetics, Mechanisms and Catalysis* **2020**, *131*, 489−503.

(9) Hu, Y.; Muhammad, T.; Wu, B.; Wei, A.; Yang, X.; Chen, L. A simple on-line detection system based on fiber-optic sensing for the realtime monitoring of fixed bed adsorption processes of molecularly imprinted polymers. *Journal of Chromatography A* **2020**, *1622*, 461112.

(10) Mandal, S.; Sarkar, B.; Igalavithana, A. D.; Ok, Y. S.; Yang, X.; Lombi, E.; Bolan, N. Mechanistic insights of 2, 4-D sorption onto biochar: Influence of feedstock materials and biochar properties. *Bioresource technology* **2017**, *246*, 160−167.

(11) Wang, J.; Zhu, J.; Si, L.; Du, Q.; Li, H.; Bi, W.; Chen, D. D. Y. High throughput screening of phenoxy carboxylic acids with dispersive solid phase extraction followed by direct analysis in real time mass spectrometry. *Analytica chimica acta* **2017**, *996*, 20−28.

(12) Mpatani, F. M.; Aryee, A. A.; Han, R.; Kani, A. N.; Li, Z.; Qu, L. Green fabrication of a novel cetylpyridinium-bagasse adsorbent for sequestration of micropollutant 2, 4-D herbicide in aqueous system and its antibacterial properties against S. aureus and E. coli. *Journal of Environmental Chemical Engineering* **2021**, *9* (6), 106714.

(13) Zhu, L.; Zhao, N.; Tong, L.; Lv, Y.; Li, G. Characterization and evaluation of surface modified materials based on porous biochar and its adsorption properties for 2, 4-dichlorophenoxyacetic acid. *Chemosphere* **2018**, *210*, 734−744.

(14) Abdelrahman, E. A.; Subaihi, A. Application of geopolymers modified with chitosan as novel composites for efficient removal of Hg (II), Cd (II), and Pb (II) ions from aqueous media. *Journal of Inorganic and Organometallic Polymers and Materials* **2020**, *30* (7), 2440−2463. Hegazey, R.; Abdelrahman, E. A.; Kotp, Y. H.; Hameed, A. M.; Subaihi, A. Facile fabrication of hematite nanoparticles from Egyptian insecticide cans for efficient photocatalytic degradation of rhodamine B dye. *Journal of Materials Research and Technology* **2020**, *9* (2), 1652−1661.

(15) Fan, L.; Miao, J.; Wang, X.; Cai, J.; Lin, J.; Chen, F.; Chen, W.; Luo, H.; Cheng, L.; An, X.; et al. Novel Al-doped UiO-66-NH2 nanoadsorbent with excellent adsorption performance for tetracycline: adsorption behavior, mechanism, and application potential. *Journal of Environmental Chemical Engineering* **2023**, *11*, 109292.

(16) Kazak, O.; Eker, Y. R.; Akin, I.; Bingol, H.; Tor, A. Green preparation of a novel red mud@ carbon composite and its application for adsorption of 2, 4-dichlorophenoxyacetic acid from aqueous solution. *Environmental Science and Pollution Research* **2017**, *24*, 23057−23068.

(17) Li, S.; Feng, F.; Chen, S.; Zhang, X.; Liang, Y.; Shan, S. Preparation of UiO-66-NH2 and UiO-66-NH2/sponge for adsorption of 2, 4-dichlorophenoxyacetic acid in water. *Ecotoxicology and Environmental Safety* **2020**, *194*, 110440.

(18) Hladik, M. L.; Roberts, A. L.; Bouwer, E. J. Removal of neutral chloroacetamide herbicide degradates during simulated unit processes for drinking water treatment. *Water research* **2005**, *39* (20), 5033−5044.

(19) Yuan, X.; Zhong, J.; Xiong, J.; Lou, W. Cysteine-functionalization zirconium-organic framework for efficient adsorption 2, 4-dichlorophenylacetic acid from water. *Journal of Environmental Chemical Engineering* **2023**, *11* (3), 110162.

(20) Li, X.; Wang, Y.; Guo, Q. Porous NH2-MIL-101 (Fe) metal organic framework for effective photocatalytic degradation of azo dye in wastewater treatment. *Heliyon* **2022**, *8* (7), No. e09942.

(21) Liédana, N.; Lozano, P.; Galve, A.; Téllez, C.; Coronas, J. The template role of caffeine in its one-step encapsulation in MOF NH 2-MIL-88B (Fe). *J. Mater. Chem. B* **2014**, *2* (9), 1144−1151.

(22) Capková, D.; Almáši, M.; Kazda, T.; Čech, O.; Király, N.; Čudek, P.; Fedorková, A. S.; Hornebecq, V. Metal-organic framework MIL-101 (Fe)−NH2 as an efficient host for sulphur storage in long-cycle Li−S batteries. *Electrochim. Acta* **2020**, *354*, 136640.

(23) Dong, Y.; Hu, T.; Pudukudy, M.; Su, H.; Jiang, L.; Shan, S.; Jia, Q. Influence of microwave-assisted synthesis on the structural and textural properties of mesoporous MIL-101 (Fe) and NH2-MIL-101 (Fe) for enhanced tetracycline adsorption. *Mater. Chem. Phys.* **2020**, *251*, 123060.

(24) Subaihi, A.; Al-Qahtani, S. D.; Attar, R. M.; Alkhamis, K.; Alzahrani, H. K.; Alhasani, M.; El-Metwaly, N. M. Preparation of fluorescent cotton fibers with antimicrobial activity using lanthanide-doped pigments. *Cellulose* **2022**, *29* (11), 6393−6404.

(25) Mogharbel, R. T.; Alkhamis, K.; Felaly, R.; El-Desouky, M.; El-Bindary, A.; El-Metwaly, N. M.; El-Bindary, M. Superior adsorption and removal of industrial dye from aqueous solution via magnetic

silver metal-organic framework nanocomposite. *Environmental Technology* **2023**, 1−17.
(26) Almahri, A.; Abou-Melha, K. S.; Katouah, H. A.; Al-bonayan, A. M.; Saad, F. A.; El-Desouky, M. G.; El-Bindary, A. A. Adsorption and removal of the harmful pesticide 2,4-dichlorophenylacetic acid from an aqueous environment via coffee waste biochar: Synthesis, characterization, adsorption study and optimization via Box-Behnken design. *J. Mol. Struct.* **2023**, *1293*, 136238. Almahri, A.; Morad, M.; Aljohani, M. M.; Alatawi, N. M.; Saad, F. A.; Abumelha, H. M.; El-Desouky, M. G.; El-Bindary, A. A. Atrazine reclamation from an aqueous environment using a ruthenium-based metal-organic framework. *Process Safety and Environmental Protection* **2023**, *177*, 52−68.
(27) Alrefaee, S. H.; Aljohani, M.; Alkhamis, K.; Shaaban, F.; El-Desouky, M. G.; El-Bindary, A. A.; El-Bindary, M. A. Adsorption and effective removal of organophosphorus pesticides from aqueous solution via novel metal-organic framework: Adsorption isotherms, kinetics, and optimization via Box-Behnken design. *J. Mol. Liq.* **2023**, *384*, 122206.
(28) Alsharief, H. H.; Alatawi, N. M.; Al-bonayan, A. M.; Alrefaee, S. H.; Saad, F. A.; El-Desouky, M. G.; El-Bindary, A. A. Adsorption of Azorubine E122 dye via Na-mordenite with tryptophan composite: batch adsorption, Box−Behnken design optimization and antibacterial activity. *Environmental Technology (United Kingdom)* **2023**, 1.
(29) Langmuir, I. The constitution and fundamental properties of solids and liquids. Part I. Solids. *J. Am. Chem. Soc.* **1916**, *38* (11), 2221−2295.
(30) Freundlich, H. M. F. Over the adsorption in solution. *J. Phys. Chem.* **1906**, *57*, 385−471.
(31) Dubinin, M. The equation of the characteristic curve of activated charcoal. *Proc. Acad. Sci. USSR Phys. Chem. Sect.* **1947**, *55*, 327−329.
(32) Tempkin, V. P. Kinetics of ammonia synthesis on promoted iron catalyst. *Acta Phys. Chim. USSR* **1940**, *12*, 327−356.
(33) Redlich, O.; Peterson, D. L. A useful adsorption isotherm. *J. Phys. Chem.* **1959**, *63* (6), 1024−1024.
(34) Mogharbel, R. T.; Alkhamis, K.; Felaly, R.; El-Desouky, M. G.; El-Bindary, A. A.; El-Metwaly, N. M.; El-Bindary, M. A. Superior adsorption and removal of industrial dye from aqueous solution via magnetic silver metal-organic framework nanocomposite. *Environmental Technology (United Kingdom)* **2023**, 1. Alsuhaibani, A. M.; Refat, M. S.; Adam, A. M. A.; El-Desouky, M. G.; El-Bindary, A. A. Enhanced adsorption of ceftriaxone antibiotics from water by mesoporous copper oxide nanosphere. *Desalination and Water Treatment* **2023**, *281*, 234−248.
(35) Al-Hazmi, G. H.; Adam, A. M. A.; El-Desouky, M. G.; ElBindary, A. A.; Alsuhaibani, A. M.; Refat, M. S. EFFICIENT ADSORPTION OF RHODAMINE B USING A COMPOSITE OF Fe3O4@ZIF-8: SYNTHESIS, CHARACTERIZATION, MODELING ANALYSIS, STATISTICAL PHYSICS AND MECHANISM OF INTERACTION. *Bulletin of the Chemical Society of Ethiopia* **2022**, *37* (1), 211−229. El-Metwaly, N. M.; Katouah, H. A.; El-Desouky, M. G.; El-Bindary, A. A.; El-Bindary, M. A. Fabricating of Fe3O4@Ag-MOF nanocomposite and evaluating its adsorption activity for removal of doxorubicin. *Journal of Environmental Science and Health - Part A Toxic/Hazardous Substances and Environmental Engineering* **2022**, *57* (13−14), 1099−1115.
(36) Lagergren, S. K. About the theory of so-called adsorption of soluble substances. *Sven. Vetenskapsakad. Handingarl* **1898**, *24*, 1−39.
(37) Ho, Y.-S.; McKay, G. Pseudo-second order model for sorption processes. *J. Process biochemistry* **1999**, *34* (5), 451−465.
(38) Wu, F.-C.; Tseng, R.-L.; Juang, R.-S. J. C. e. j. Initial behavior of intraparticle diffusion model used in the description of adsorption kinetics. *J. Chem. eng. j.* **2009**, *153* (1−3), 1−8.
(39) Vlad, M.; Segal, E. A kinetic analysis of Langmuir model for adsorption within the framework of Jovanovic theory; a generalization of the Jovanovic isotherm. *J. Surf. Sci.* **1979**, *79* (2), 608−616.
(40) El-Desouky, M. G.; Shahat, A.; El-Bindary, A. A.; El-Bindary, M. A. Description, kinetic and equilibrium studies of the adsorption of carbon dioxide in mesoporous iron oxide nanospheres. *Biointerface Research in Applied Chemistry* **2021**, *12* (1), 1022−1038.
(41) El-Desouky, M. G.; Khalil, M. A. G.; El-Afify, M. A. M.; El-Bindary, A. A.; El-Bindary, M. A. Effective methods for removing different types of dyes − modelling analysisstatistical physics treatment and DFT calculations: a review. *Desalination and Water Treatment* **2022**, *280*, 89−127. El-Desouky, M. G.; Khalil, M. A.; El-Bindary, A. A.; El-Bindary, M. A. Biological, biochemical and thermochemical techniques for biofuel production: An updated review. *Biointerface Research in Applied Chemistry* **2021**, *12* (3), 3034−3054.
(42) El-Desouky, M. G.; El-Bindary, M. A.; El-Bindary, A. A. Effective adsorptive removal of anionic dyes from aqueous solution. *Vietnam Journal of Chemistry* **2021**, *59* (3), 341−361.
(43) El-Desouky, M. G.; El-Bindary, A. A. Magnetic metal-organic framework (Fe3O4@ZIF-8) nanocomposites for adsorption of anionic dyes from wastewater. *Inorganic and Nano-Metal Chemistry* **2021**, 1.
(44) El-Bindary, M. A.; El-Desouky, M. G.; El-Bindary, A. A. Metal−organic frameworks encapsulated with an anticancer compound as drug delivery system: Synthesis, characterization, antioxidant, anticancer, antibacterial, and molecular docking investigation. *Appl. Organomet. Chem.* **2022**, DOI: 10.1002/aoc.6660.
(45) Al-Wasidi, A. S.; AlZahrani, I. I. S.; Thawibaraka, H. I.; Naglah, A. M.; El-Desouky, M. G.; El-Bindary, M. A. Adsorption studies of carbon dioxide and anionic dye on green adsorbent. *J. Mol. Struct.* **2022**, *1250*, 131736.
(46) El-Desouky, M. G.; El-Bindary, A. A.; El-Afify, M. A. M.; Hassan, N. Synthesis, characterization, theoretical calculation, DNA binding, molecular docking, anticovid-19 and anticancer chelation studies of some transition metal complexes. *Inorganic and Nano-Metal Chemistry* **2022**, *52* (9), 1273−1288.
(47) Altalhi, T. A.; Ibrahim, M. M.; Mersal, G. A.M.; Mahmoud, M.H.H.; Kumeria, T.; El-Desouky, M. G.; El-Bindary, A. A.; El-Bindary, M. A. Adsorption of doxorubicin hydrochloride onto thermally treated green adsorbent: Equilibrium, kinetic and thermodynamic studies. *J. Mol. Struct.* **2022**, *1263*, 133160.
(48) Alsuhaibani, A. M.; Refat, M. S.; Atta, A. A.; El-Desouky, M. G.; El-Bindary, A. A. Efficient adsorption and removal of tetracycline antibiotics from aqueous solutions onto nickel oxide nanoparticles via organometallic chelate. *Desalination and Water Treatment* **2022**, *277*, 190−205. Al-Hazmi, G. H.; Refat, M. S.; El-Desouky, M. G.; Wali, F. K. M.; El-Bindary, A. A. Effective removal of industrial dye from aqueous solution using mesoporous nickel oxide: a complete batch system evaluation. *Desalination and Water Treatment* **2022**, *273*, 246−260.
(49) Al-Hazmi, G. H.; Refat, M. S.; El-Desouky, M. G.; El-Bindary, A. A. Effective adsorption and removal of industrial dye from aqueous solution using mesoporous zinc oxide nanoparticles via metal organic frame work: equilibrium, kinetics and thermodynamic studies. *Desalination and Water Treatment* **2022**, *272*, 277−289. Al-Hazmi, G. H.; El-Desouky, M. G.; El-Bindary, A. A. SYNTHESIS, CHARACTERIZATION AND MICROSTRUCTURAL EVALUATION OF ZnO NANOPARTICLES BY WILLIAM-HALL AND SIZE-STRAIN PLOT METHODS. *Bulletin of the Chemical Society of Ethiopia* **2022**, *36* (4), 815−829. Al-Hazmi, G. A. A.; El-Zahhar, A. A.; El-Desouky, M. G.; El-Bindary, M. A.; El-Bindary, A. A. Adsorption of industrial dye onto a zirconium metal-organic framework: synthesis, characterization, kinetics, thermodynamics, and DFT calculations. *J. Coord. Chem.* **2022**, *75* (9−10), 1203−1229.
(50) Hassan, N.; Shahat, A.; El-Didamony, A.; El-Desouky, M. G.; El-Bindary, A. A. Synthesis and characterization of ZnO nanoparticles via zeolitic imidazolate framework-8 and its application for removal of dyes. *J. Mol. Struct.* **2020**, *1210*, 128029.

https://doi.org/10.1021/acsomega.3c05818
ACS Omega 2023, 8, 40775−40784